2011

In situ Transmission Electron Microscopy Study on the Phase Transitionsin Lead-Free (1–x)(Bi1/2Na1/2)TiO3–xBaTiO3 Ceramics

C. Ma
Iowa State University

Xiaoli Tan
Iowa State University, xtan@iastate.edu

In situ Transmission Electron Microscopy Study on the Phase Transitionsin Lead-Free (1–x)(Bi1/2Na1/2)TiO3–xBaTiO3 Ceramics

Abstract
The phase transitions in unpoled lead-free $(1-x)(Bi_{1/2}Na_{1/2})TiO_3-xBaTiO_3$ (x = 0.06 and 0.11) ceramics are investigated using hot-stage transmission electron microscopy (TEM). It is found that large ferroelectric domains in both ceramics start to disappear around T_d, the depolarization temperature. After the transition, both compositions exhibit the *P4bm* tetragonal symmetry in the form of nanodomains. The structural transition observed by the *in situ*TEM experiments seems to be gradual and occurs within a temperature range of several tens of degrees, in contrast to the sharp anomaly at T_d revealed by the dielectric characterization. With further increasing temperature, no structural change was observed for both compositions across T_{RE}, where the dielectric frequency dispersion vanishes, and T_m, where the dielectric permittivity reaches maximum. The tetragonal-to-cubic transition is diffuse and takes place in a broad temperature window well above both T_{RE} and T_m. These results of structural phase transitions are summarized in a phase diagram with its composition range covering the morphotropic phase boundary (MPB).

Keywords
Lead-free piezoelectrics, domain structure, phase transition, transmission electron microscopy

Disciplines
Ceramic Materials | Power and Energy | Tribology

Comments
This is the peer reviewed version of the following article: Journal of the American Ceramic Society 94, 4040-4044 (2011). DOI: 10.1111/j.1551-2916.2011.04670.x.

In situ Transmission Electron Microscopy Study on the Phase Transitions in Lead-Free $(1-x)(Bi_{1/2}Na_{1/2})TiO_3$–$xBaTiO_3$ Ceramics

C. Ma and X. Tan*,¶

Department of Materials Science and Engineering, Iowa State University, Ames, IA 50011, USA

This work was supported by the National Science Foundation (NSF) through Grant DMR-1037898.

TEM experiments were performed at the Ames Laboratory which is operated for the U.S. Department of Energy by Iowa State University under Contract No. DE-AC02-07CH11358.

*Member, the American Ceramic Society.

¶Author to whom correspondence should be addressed. Electronic mail: xtan@iastate.edu

Abstract

The phase transitions in unpoled lead-free (1-x)($Bi_{1/2}Na_{1/2}$)TiO_3–$x$$BaTiO_3$ (x = 0.06 and 0.11) ceramics are investigated using hot-stage transmission electron microscopy (TEM). It is found that large ferroelectric domains in both ceramics start to disappear around T_d, the depolarization temperature. After the transition, both compositions exhibit the *P4bm* tetragonal symmetry in the form of nanodomains. The structural transition observed by the *in situ* TEM experiments seems to be gradual and occurs within a temperature range of several tens of degrees, in contrast to the sharp anomaly at T_d revealed by the dielectric characterization. With further increasing temperature, no structural change was observed for both compositions across T_{RE}, where the dielectric frequency dispersion vanishes, and T_m, where the dielectric permittivity reaches maximum. The tetragonal-to-cubic transition is diffuse and takes place in a broad temperature window well above both T_{RE} and T_m. These results of structural phase transitions are summarized in a phase diagram with its composition range covering the morphotropic phase boundary (MPB).

Keywords: Lead-free piezoelectrics, domain structure, phase transition, transmission electron microscopy

I. Introduction

The development of high-performance lead-free piezoelectric ceramics becomes an increasingly urgent task because of the environmental concerns raised by lead-containing piezoelectric ceramics such as $Pb(Zr,Ti)O_3$.[1] The $(1-x)(Bi_{1/2}Na_{1/2})TiO_3$–$xBaTiO_3$ solid solution system, whose piezoelectric properties peak at its morphotropic phase boundary (MPB) $x \approx 0.06$, has shown great promises for piezoelectric applications.[1-4] However, several fundamental issues, especially those on the structure-property relationships, are not very well understood in this system and the origin of the piezoelectric strain is still unclear.[5] The complications regarding the structure-property relationships in $(1-x)(Bi_{1/2}Na_{1/2})TiO_3$–$xBaTiO_3$ can be traced back to the base compound $(Bi_{1/2}Na_{1/2})TiO_3$, which displays decoupled crystal structures and dielectric properties.[6-9] Neutron diffraction experiments[7] indicate that $(Bi_{1/2}Na_{1/2})TiO_3$ exhibits *R3c* symmetry below 255 ºC, *P4bm* symmetry from 400 to 500 ºC, and $Pm\bar{3}m$ symmetry above 540 ºC. The *R3c* and *P4bm* phases coexist between 255 ºC and 400 ºC, and the *P4bm* and $Pm\bar{3}m$ phases coexist between 500 ºC and 540 ºC. Structural refinements suggest that the tetragonal *P4bm* phase exhibits Ti^{4+} displacements antiparallel to those of Bi^{3+}/Na^{+}.[7] However, dielectric characterizations reveal that the room-temperature ferroelectric state in $(Bi_{1/2}Na_{1/2})TiO_3$ transforms to an antiferroelectric state at ~230 ºC (T_d) where a hump in dielectric constant and loss tangent was observed, and then to a paraelectric one at ~340 ºC (T_m) where dielectric constant exhibits a maximum.[2] The disconnection between the structural and the dielectric transitions is poorly understood.

The dielectric phase transitions in $(Bi_{1/2}Na_{1/2})TiO_3$ are inherited by the MPB compositions of $(1-x)(Bi_{1/2}Na_{1/2})TiO_3–xBaTiO_3$,[2-4,10] but the structure-property relationship against temperature is unknown due to the absence of systematic temperature dependent structural studies. In the recently reported phase diagram for unpoled $(1-x)(Bi_{1/2}Na_{1/2})TiO_3–xBaTiO_3$ ceramics (Fig. 1),[11,12] excellent structure-property correlation against composition was observed at room temperature. The unique relaxor antiferroelectric (AFE) behavior is associated with nanodomains with *P4bm* symmetry in the phase region $0.07 \leq x \leq 0.09$, and long-range ferroelectric (FE) order was observed in both neighboring phase regions with large ferroelectric domains. The MPB composition $x = 0.06$ displays a two-phase mixture with volumes of *R3c* ferroelectric domains embedded in the matrix of *P4bm* nanodomains, while the composition $x = 0.11$ contains both *P4bm* nanodomains and *P4mm* large lamellar ferroelectric domains. Based on the excellent structure-property correlation at room temperature, it was further speculated that the *R3c* complex domains in $x \leq 0.06$ and the *P4mm* lamellar domains in $x \geq 0.11$ transform to the *P4bm* nanodomains across T_d, the dielectric anomaly delineating the FE and relaxor AFE regions in Fig. 1.[11,12] Given the aforementioned complications arising from the decoupled dielectric and structural transitions in $(Bi_{1/2}Na_{1/2})TiO_3$,[6-9] experimental evidences are needed to verify this speculation. In addition, the structure-property relationship across T_{RE}, where the dielectric frequency dispersion vanishes,[11,12] and T_m, where the dielectric permittivity peaks,[2] is unknown for the compositions around the MPB. It has been proposed that T_{RE} may not correspond to a structural change.[12]

As for T_m, a recent study suggests that the tetragonal-cubic transition temperature drops towards T_m with increasing x, and these two transition temperatures start to converge in $x = 0.05$.[10] For $x > 0.05$, though, the anelastic anomaly caused by the tetragonal-cubic transition becomes extremely broadened, which prevents accurate determination of the structural transition temperature.[10] Whether the tetragonal-cubic transition temperature merges with T_m, and how the domain structure evolves with temperature above T_m for $x > 0.05$ thus remain open questions. In the present work, hot-stage transmission electron microscopy (TEM) study was performed on ceramics of $x = 0.06$ and 0.11 to reveal the structural transitions.

II. Experimental Procedure

The preparation of $(1-x)(Bi_{1/2}Na_{1/2})TiO_3–xBaTiO_3$ polycrystalline ceramics and TEM specimens was reported previously.[11,12] Hot-stage TEM experiments on ceramic specimens of $x = 0.06$ and 0.11 were performed on a Phillips CM-30 microscope operated at 300 kV. Bright field micrographs, centered-dark-field (CDF) micrographs, and selected area electron diffraction (SAED) patterns were recorded with a charge-coupled device camera during specimen heating. The temperature was increased in a stepwise manner with a step size ~20 ºC and each step took ~1 minute. At temperature points of interest, TEM micrographs and/or diffraction patterns were recorded 10 minutes after the temperature reading was stabilized. Due to the concern of possible evaporation loss of Bi^{3+} and Na^{+}, all specimens were heated to a temperature at or below 600 ºC and the whole heating experiment was finished within 3 hours.

III. Results and Discussion

(1). Phase transitions across T_d

In agreement with previous results,[11,12] ~40 % of the grains in the composition $x = 0.06$ at room temperature exhibit the mixed-phase structure with volumes of complex ferroelectric domains embedded in the matrix of nanodomains, and the rest of the grains contain nanodomains only. Figure 2(a) displays the room-temperature bright field image of a grain with the mixed-phase structure along the [112] zone axis. The volume in the center of the micrograph is occupied by ferroelectric domains in a complex pattern. These domains exhibit the *R3c* symmetry as characterized by the presence of strong $\frac{1}{2}\{ooo\}$ and absence of $\frac{1}{2}\{ooe\}$ superlattice spots [Fig. 2(b)] (*o* and *e* denotes odd and even Miller indices, respectively).[13-15] The nanodomains in the volume surrounding the *R3c* ferroelectric domains possess the *P4bm* symmetry as evidenced by the presence of $\frac{1}{2}\{ooe\}$ and absence of $\frac{1}{2}\{ooo\}$ spots [Fig. 2(c)].[7,8,13-15]

With increasing temperature, the volume containing the complex ferroelectric domains starts to shrink at around 130 ºC and this process continues until ~170 ºC where the whole grain is completely occupied by nanodomains with the *P4bm* symmetry. Figure 2(d) depicts the morphology of the volume with *R3c* ferroelectric domains at 140 ºC. Obviously the *R3c* $\rightarrow$ *P4bm* structural phase transition takes place through the motion of the interphase boundary: The volume with *P4bm* nanodomains expands at the expense of the volume with the *R3c* complex

ferroelectric domains and finally occupies the whole grain above 170 ºC [Fig. 2(e)]. Figures 2(f) and 2(g) display the SAED patterns recorded at 190 ºC from the volume originally occupied by *R3c* ferroelectric domains and from the surrounding volume, respectively. Both show identical diffraction patterns with apparent $\frac{1}{2}\{ooe\}$ spots.

We have proposed a new term "relaxor antiferroelectric" to describe the dielectric behavior of the *P4bm* phase for its strong frequency dispersion and its nanometer-sized domains in our previous work.[11,12] It is in analogy with "relaxor ferroelectric" which has been used to describe $Pb(Mg_{1/3}Nb_{2/3})O_3$ where the nanodomains are ferroelectric ones.[16-18] For the "relaxor antiferroelectric" *P4bm* phase in $(1-x)(Bi_{1/2}Na_{1/2})TiO_3–xBaTiO_3$, the nanodomains are of antiferroelectric nature because the displacements of A-site cations (Bi^{3+}, Na^{+}, Ba^{2+}) are antiparallel to the displacement of B-site cation (Ti^{4+}) within each individual nanodomain. However, the dipole moment resulted from the Ti^{4+} displacement is not fully cancelled by that from the A-site cation displacement in the unit cell.[7] Therefore, the nanodomains in the *P4bm* phase are actually uncompensated antiferroelectric, or weakly polar ferrielectric domains.[12] As a result, the dielectric behavior of the *P4bm* relaxor antiferroelectric phase is similar to that of a relaxor ferroelectric in many aspects.[12]

For the unpoled ceramic of $x = 0.06$, dielectric measurements indicated that T_d is 115 ºC (Fig. 1).[11,12] Considering the difference in the sample geometry for dielectric and TEM characterizations and the accuracy in the temperature reading for hot-stage TEM experiments, the observed *R3c*-to-*P4bm* structural phase transition from the *in situ* TEM study seems to

correlate with the ferroelectric-to-relaxor-antiferroelectric transition at T_d from the dielectric characterization.

Similar results were observed in $x = 0.11$ (Fig. 3). At room temperature, the unpoled ceramic is dominated by lamellar ferroelectric domains [Fig. 3(a)]. Figure 3(b) is the SAED pattern along the [112] zone axis recorded from the area in the lower left portion of the grain where nanodomains are observed [indicated by the bright arrow in Fig. 3(a)]. The presence of weak $\frac{1}{2}\{ooe\}$ and absence of $\frac{1}{2}\{ooo\}$ superlattice spots confirm the *P4bm* symmetry.[7,8,13-15] As shown in Fig. 3(c), the large lamellar domains exhibit the *P4mm* symmetry as characterized by the absence of any superlattice spots. During heating, the volume with *P4bm* nanodomains started to grow at the expense of lamellar domains at 170 ºC and all the lamellar domains in the grain disappeared at 240 ºC. Figure 3(e) displays the bright field micrograph recorded at 250 ºC for the same grain where faint contrast of nanodomains is evident. The $\frac{1}{2}\{ooe\}$ superlattice spots, although very weak, are still visible at this temperature (see the inset). Therefore, the *P4mm* $\rightarrow$ *P4bm* structural transition appears to correlate well with the dielectric transition at T_d, which is 170 ºC for $x = 0.11$ (Fig. 1).[11,12]

The present *in situ* TEM study demonstrates that the temperature T_d not only marks the ferroelectric-to-relaxor-antiferroelectric phase transition, but also corresponds to structural changes in the $(1-x)(Bi_{1/2}Na_{1/2})TiO_3$–$xBaTiO_3$ binary solid solution system. The results are hence in supportive of the phase diagram we proposed previously for unpoled ceramics.[11,12] However, it should be noted that the dielectric transition at T_d is sharp while the structural

transition revealed by *in situ* TEM experiments takes place over a wide temperature window of several tens of degrees. Although exact reasons for this discrepancy are the subject for future studies, the different sample geometry and in turn the different electromechanical boundary conditions definitely are contributing factors.

(2). Transitions across and beyond T_{RE} and T_m

More detailed hot-stage TEM study was performed on the nanodomains in x = 0.06 and 0.11 in order to investigate the domain structures at high temperatures up to 600 ºC. Figure 4 displays the CDF image of the nanodomains in x = 0.06 at room temperature, which was formed with the $\frac{1}{2}(3\bar{1}0)$ superlattice diffraction spot in the $[130]_c$ zone axis. The CDF micrograph reveals that the nanodomains (bright speckles) took a thin platelet shape parallel to the (001) plane, which causes streaking of $\frac{1}{2}\{ooe\}$ diffraction spots along the [001] direction (inset of Fig. 4). The matrix with dark contrast should be a mixture of nanodomains of other variants and the cubic perovskite phase.[12] No detectable change in the shape, size, or population of the nanodomains was observed from room temperature up to 335 ºC. Dark field imaging was not performed beyond 335 ºC due to the severe drifting and weak contrast.

Figure 5 displays the $[130]_c$ zone axis SAED patterns in x = 0.06 recorded from the volume occupied by nanodomains at a series of temperatures. The characteristic feature of the *P4bm* symmetry, *i.e.* the presence of $\frac{1}{2}\{ooe\}$ and absence of $\frac{1}{2}\{ooo\}$ superlattice spots, persists to temperatures well beyond T_m, which is ~280 °C for x = 0.06.[12] The SAED pattern

does not exhibit any significant change up to 335 ºC [Fig. 5(a) and (b)]. Gradual weakening of the $\frac{1}{2}\{ooe\}$ spots was observed above 335 ºC, as exemplified by the SAED pattern recorded at 425 ºC [Fig. 5(c)]. This indicates that the tetragonal-to-cubic structural transition started to occur at 335 ºC. Above 335 ºC, the $\frac{1}{2}\{ooe\}$ spots become more diffused and severely streaking with increasing temperature, suggesting that the size, in addition to the population, of the *P4bm* nanoplatelets is also decreasing during the structural transition. When the temperature reached 500 ºC, as shown in Fig. 5(d), only weak residues of the $\frac{1}{2}\{ooe\}$ spots were observed and they remained, although barely detectable, even at 600 ºC. The *in situ* TEM results thus suggest that the tetragonal (*P4bm*) to cubic structural transition starts at 335 ºC and completes at 500 ºC. However, the high-temperature phase (at least between 500 and 600 ºC) seems not to be a "clean" cubic phase. The persistent residues of $\frac{1}{2}\{ooe\}$ superlattice spots, which have also been observed in pure $(Bi_{1/2}Na_{1/2})TiO_3$ up to 620 ºC,[19] reveal the presence of local lattice distortions. It should be noted that local lattice distortions in an average cubic structure has previously been revealed by the x-ray absorption fine structure in pure $(Bi_{1/2}Na_{1/2})TiO_3$ at 600 ºC.[20] Note that T_{RE} and T_m for $x = 0.06$ are 240 ºC and 280 ºC, respectively (Fig. 1), from dielectric measurements.[11,12] The lack of obvious changes in either the domain morphology or the superlattic diffraction spots up to 335 ºC from this study indicates that the dielectric anomalies at T_{RE} and T_m do not correspond to any structural phase transitions. The tetragonal-to-cubic structural transition occurs progressively between 335 ºC and 500 ºC.

Figure 6 displays the SAED patterns of nanodomains in $x = 0.11$ at different temperatures. Similar to $x = 0.06$, the SAED patterns exhibit $\frac{1}{2}\{ooe\}$ superlattice spots without $\frac{1}{2}\{ooo\}$ ones. The $\frac{1}{2}(\bar{3}10)$ superlattice diffraction spot from the nanodomains was very weak even at room temperature for $x = 0.11$ [Fig. 6(a)], so the CDF image was not recorded. The bright field images (not shown here) could not reveal any obvious morphology change of nanodomains from room temperature to 600 ºC. The superlattice spots with streaking at all temperatures studied suggest a thin platelet domain morphology of the *P4bm* phase, which is similar to that in $x = 0.06$ (Fig. 4). Weakening in the $\frac{1}{2}\{ooe\}$ superlattice spots is noted at 310 ºC [Fig. 6(b)]. However, these superlattice spots are still discrete and can be distinguished from background at this temperature. As the temperature further increased, the superlattice spots are more dramatically elongated and diffused [Fig. 6(c)]. At 425 ºC, the superlattice diffractions become so weak and streaked that they can hardly be distinguished as individual spots [Fig. 6(d)]. No significant change was observed in the SAED patterns with increasing temperature above 425 ºC, except the slow and gradual weakening of the diffuse residues of the superlattice diffractions. These residues are still visible up to 550 ºC and eventually cannot be well recorded at 600 ºC. Thus the *in situ* TEM study suggests that the tetragonal-to-cubic structural transition starts at a temperature slightly below 310 °C and finishes at 425 °C in the composition of $x = 0.11$. The local distortions in the high-temperature cubic phase are gradually weakening with increase in temperature and persist up to at least 550 °C. The dielectric transition temperatures T_{RE} and T_m for $x = 0.11$ are 255 and 275 ºC, respectively (Fig. 1).[11,12] Again, neither of them is associated

with the tetragonal-to-cubic structural phase transition according to the present hot-stage TEM study.

Summarizing the results of this study and previous work,[10-12] a schematic phase diagram accounting for the structural phase transitions in unpoled $(1-x)(Bi_{1/2}Na_{1/2})TiO_3–xBaTiO_3$ ceramics can be constructed (Fig. 7). While the dielectric anomaly T_d correlates well with the structural transition to the *P4bm* phase, the dielectric anomalies at T_{RE} and T_m do not correspond to any structural phase transition. The tetragonal-to-cubic structural transition takes place progressively within a wide temperature range above T_m where both the size and the population of the platelets of *P4bm* nanodomains decrease with increasing temperature. The extremely weak residues of $\frac{1}{2}\{ooe\}$ superlattice diffractions observed after this structural transition reveals the presence of local lattice distortions in the high-temperature cubic phase, similar to those in pure $(Bi_{1/2}Na_{1/2})TiO_3$.[20] However, the gradual weakening of these residues after the structural transition appears to suggest such distortion may eventually disappear at higher temperatures. This scenario agrees with previous anelasticity measurement results which indicate a broad and diffuse tetragonal-to-cubic transition above T_m in compositions of $x \geq 0.05$.[10]

IV. Conclusions

In summary, structural phase transitions in unpoled $(1-x)(Bi_{1/2}Na_{1/2})TiO_3–xBaTiO_3$ ceramics were investigated using hot-stage TEM. The dielectric transition at T_d is found to be correlated with structural transitions to a *P4bm* tetragonal phase. Nanodomains with the *P4bm*

symmetry are confirmed in compositions of $x = 0.06$ and 0.11 at temperatures above T_d. With further increase in temperature, no structural phase transition is observed to occur at T_{RE} or T_m. The tetragonal-to-cubic phase transition takes place progressively within a wide temperature range above T_m: from 335 ºC to 500 ºC in $x = 0.06$ and from a temperature slightly below 310 ºC to 425 ºC in $x = 0.11$. Local distortions are present in the high-temperature cubic phase after the tetragonal-to-cubic structural transition and persist to temperatures close to 600 °C. Such local distortions are expected to eventually vanish with further increase in temperature.

References

[1] J. Rödel, W. Jo, K. Seifert, E.M. Anton, T. Granzow, and D. Damjanovic, "Perspective on the Development of Lead-Free Piezoceramics," *J. Am. Ceram. Soc.*, **92**, 1153 (2009).

[2] T. Takenaka, K. Maruyama, and K. Sakata, "$(Bi_{1/2}Na_{1/2})TiO_3$–$BaTiO_3$ System for Lead-Free Piezoelectric Ceramics," *Jpn. J. Appl. Phys.*, Part 1 **30**, 2236 (1991).

[3] Y. Hiruma, Y. Watanabe, H. Nagata, and T. Takenaka, "Phase Transition Temperatures of Divalent and Trivalent Ions Substituted $Bi_{0.5}Na_{0.5}TiO_3$ Ceramics," *Key Eng. Mater.*, **350,** 93 (2007).

[4] C. Xu, D. Lin, and K.W. Kwok, "Structure, Electrical Properties and Depolarization Temperature of $(Bi_{0.5}Na_{0.5})TiO_3$-$BaTiO_3$ Lead-Free Piezoelectric Ceramics," *Solid State Sci.*, **10**, 934 (2008).

[5] J.E. Daniels, W. Jo, J. Rödel, and J.L. Jones, "Electric-Field-Induced Phase Transformation at a Lead-Free Morphotropic Phase Boundary: Case Study in a 93%$(Bi_{0.5}Na_{0.5})TiO_3$–7%$BaTiO_3$ Piezoelectric Ceramic," *Appl. Phys. Lett.*, **95**, 032904 (2009).

[6] C.S. Tu, I.G. Siny, and V.H. Schmidt, "Sequence of Dielectric Anomalies and High-Temperature Relaxation Behavior in $Na_{1/2}Bi_{1/2}TiO_3$," *Phys. Rev. B*, **49**, 11550 (1994).

[7] G.O. Jones, and P.A. Thomas, "Investigation of the Structure and Phase Transitions in the Novel A-site Substituted Distorted Perovskite Compound $Na_{0.5}Bi_{0.5}TiO_3$," *Acta Cryst.*, **B58**, 168 (2002).

[8] V. Dorcet, G. Trolliard, and P. Boullay, "Reinvestigation of Phase Transitions in $Na_{0.5}Bi_{0.5}TiO_3$ by TEM. Part I: First Order Rhombohedral to Orthorhombic Phase Transition," *Chem. Mater.*, **20**, 5061 (2008).

[9] J. Yao, W. Ge, L. Luo, J. Li, D. Viehland, and H. Luo, "Hierarchical Domains in $Na_{1/2}Bi_{1/2}TiO_3$ Single Crystals: Ferroelectric Phase Transformations within the Geometrical Restrictions of a Ferroelastic Inheritance," *Appl. Phys. Lett.*, **96**, 222905 (2010).

[10] F. Cordero, F. Craciun, F. Trequattrini, E. Mercadelli, and C. Galassi, "Phase Transitions and Phase Diagram of the Ferroelectric Perovskite $(Na_{0.5}Bi_{0.5})_{1-x}Ba_xTiO_3$ by Anelastic and Dielectric Measurements," *Phys. Rev. B*, **81**, 144124 (2010).

[11] C. Ma, and X. Tan, "Phase Diagram of Unpoled Lead-Free (1-*x*)$(Bi_{1/2}Na_{1/2})TiO_3$–*x*$BaTiO_3$ Ceramics," *Solid State Commun.*, **150**, 1497 (2010).

[12] C. Ma, X. Tan, E. Dul'kin, and M. Roth, "Domain Structure-Dielectric Property Relationship in Lead-Free (1-*x*)$(Bi_{1/2}Na_{1/2})TiO_3$–*x*$BaTiO_3$ Ceramics," *J. Appl. Phys.*, **108**, 104105 (2010).

[13] D.I. Woodward, and I.M. Reaney, "Electron Diffraction of Tilted Perovskites," *Acta Cryst.*, **B61**, 387 (2005).

[14] A.M. Glazer, "Simple Ways of Determining Perovskite Structures," *Acta Cryst.*, **A31**, 756 (1975).

[15] L.A. Schmitt, and H.J. Kleebe, "Single Grains Hosting Two Space Groups – a Transmission Electron Microscopy Study of a Lead-Free Ferroelectric," *Funct. Mater. Lett.*, **3**, 55 (2010).

[16] L.E. Cross, "Relaxor Ferroelectrics," *Ferroelectrics*, **76**, 241 (1987).

[17] X. Zhao, W. Qu, H. He, N. Vittayakorn, and X. Tan, "Influence of Cation Order on the Electric Field-Induced Phase Transition in $Pb(Mg_{1/3}Nb_{2/3})O_3$-Based Relaxor Ferroelectrics," *J. Am. Ceram. Soc.*, **89**, 202 (2006).

[18] X. Zhao, W. Qu, X. Tan, A. Bokov, and Z.-G. Ye, "Electric Field-Induced Phase Transitions in (111)-, (110)-, and (100)-Oriented $Pb(Mg_{1/3}Nb_{2/3})O_3$ Single Crystals," *Phys. Rev. B*, **75**, 104106 (2007).

~~16~~19 G. Trolliard, and V. Dorcet, "Reinvestigation of Phase Transitions in $Na_{0.5}Bi_{0.5}TiO_3$ by TEM. Part II: Second Order Orthorhombic to Tetragonal Phase Transition," *Chem. Mater.*, **20**, 5074 (2008).

[20] V.A. Shuvaeva, D. Zekria, A.M. Glazer, Q. Jiang, S.M. Weber, P. Bhattacharya, and P.A. Thomas, "Local Structure of the Lead-Free Relaxor Ferroelectric $(K_xNa_{1-x})_{0.5}Bi_{0.5}TiO_3$," *Phys. Rev. B*, **71**, 174114 (2005).

Fig. 1. The phase diagram for unpoled (1-*x*)($Bi_{1/2}Na_{1/2}$)TiO_3–*x*$BaTiO_3$ ceramics.[12] Note that the transition temperatures are determined from dielectric characterizations rather than structural analysis. The dielectric constant and loss tangent curves of the compositions with $0.04 \leq x \leq 0.11$, including the two compositions for the *in situ* TEM study here, were reported in Ref. 12.

Fig. 2. *In situ* TEM experiment on the 0.94($Bi_{1/2}Na_{1/2}$)TiO_3–0.06$BaTiO_3$ ceramic along the [112] zone axis. (a) The bright field micrograph at 25 ºC; (b) the SAED pattern recorded at 25 ºC from the volume with complex ferroelectric domains in the central portion of (a); (c) the SAED pattern recorded at 25 ºC from the surrounding volume in the grain with relaxor antiferroelectric nanodomains; (d) the same grain at 140 ºC; (e) the same grain at 190 ºC; (f) the SAED pattern recorded at 190 ºC from the volume originally occupied by complex ferroelectric domains; (g) the SAED pattern recorded at 190 ºC from the surrounding volume.

Fig. 3. *In situ* TEM experiment on the 0.89($Bi_{1/2}Na_{1/2}$)TiO_3–0.11$BaTiO_3$ ceramic along the [112] zone axis. (a) The bright field micrograph at 25 ºC; (b) the SAED pattern recorded at 25 ºC from the volume occupied by relaxor antiferroelectric nanodomains [indicated by the bright arrow in (a)]; (c) the SAED pattern recorded at 25 ºC from the volume with large lamellar domains in the grain; (d) the same grain at 200 ºC; and (e) the same grain at 250 ºC. The inset in (e) shows the SAED pattern recorded at 250 ºC.

Fig. 4. Centered-dark-field image of the relaxor antiferroelectric nanodomains in the $0.94(Bi_{1/2}Na_{1/2})TiO_3$–$0.06BaTiO_3$ ceramic at room temperature. The image was formed using the $\frac{1}{2}(\bar{3}10)$ superlattice diffraction spot in the $[130]_c$ zone-axis. The inset shows the SAED pattern with the $\frac{1}{2}(\bar{3}10)$ spot circled.

Fig. 5. The $[130]_c$ zone-axis SAED patterns of the nanodomains in the $0.94(Bi_{1/2}Na_{1/2})TiO_3$–$0.06BaTiO_3$ ceramic at (a) room temperature, (b) 335 ºC, (c) 425 ºC, (d) 500 ºC.

Fig. 6. The $[130]_c$ zone-axis SAED patterns of the nanodomains in the $0.89(Bi_{1/2}Na_{1/2})TiO_3$–$0.11BaTiO_3$ ceramic recorded at (a) room temperature, (b) 310 ºC, (c) 360 ºC, (d) 425 ºC.

Fig. 7. A schematic phase diagram for structural phase transitions in unpoled $(1-x)(Bi_{1/2}Na_{1/2})TiO_3$–$xBaTiO_3$ ceramics. The thick solid and dash-dot lines (colored) delineate the structural phase regions. For comparison, the temperatures for dielectric anomalies (T_d, T_{RE}, T_m) are included as dark dashed lines.

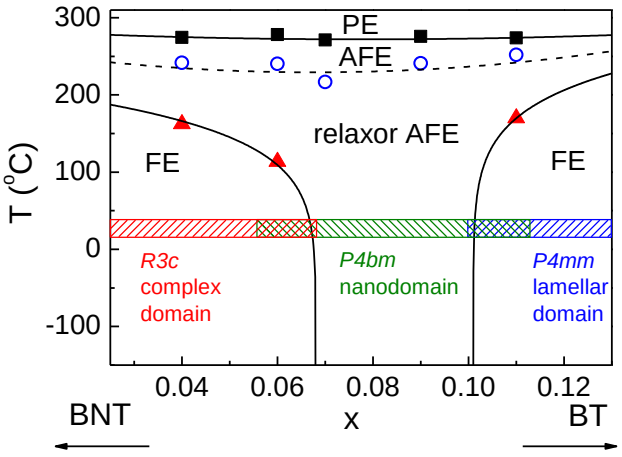
300
200
100
0
-100
T (°C)
PE
AFE
relaxor AFE
FE
FE
R3c
complex
domain
P4bm
nanodomain
P4mm
lamellar
domain
0.04
0.06
0.08
0.10
0.12
x
BNT
BT

Fig. 1

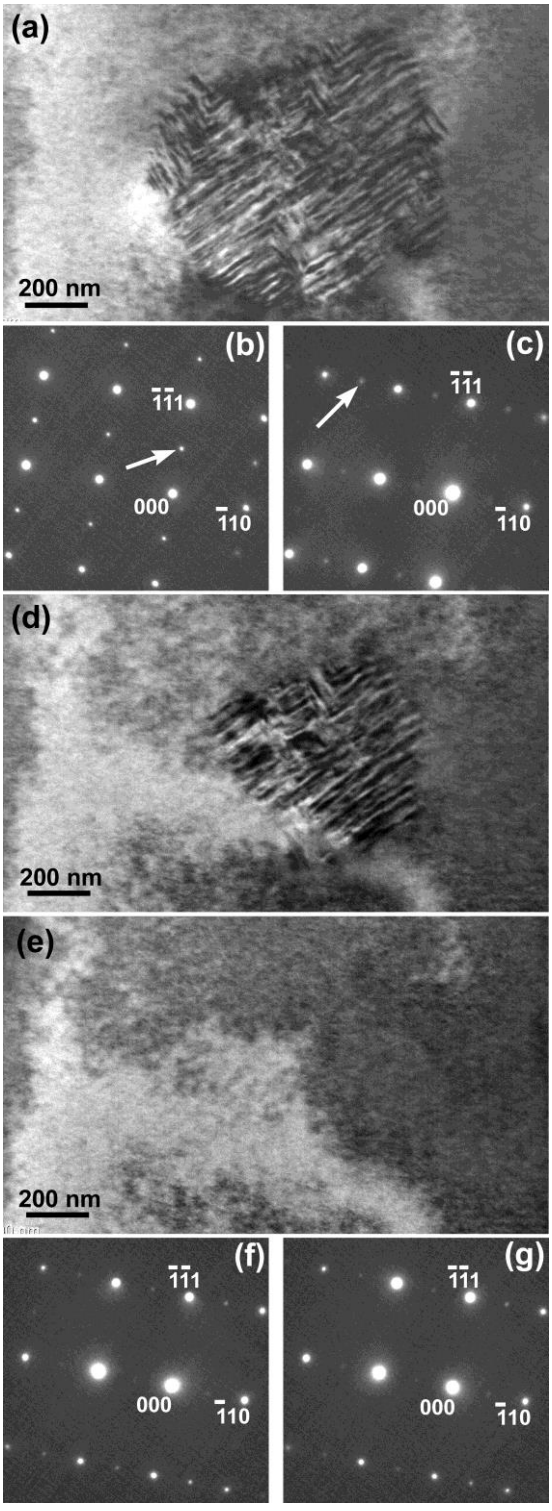
(a)
200 nm
(b)
$\bar{1}\bar{1}\bar{1}$
000
$\bar{1}\bar{1}0$
(c)
$\bar{1}\bar{1}\bar{1}$
000
$\bar{1}\bar{1}0$
(d)
200 nm
(e)
200 nm
(f)
$\bar{1}\bar{1}\bar{1}$
000
$\bar{1}\bar{1}0$
(g)
$\bar{1}\bar{1}\bar{1}$
000
$\bar{1}\bar{1}0$

Fig. 2

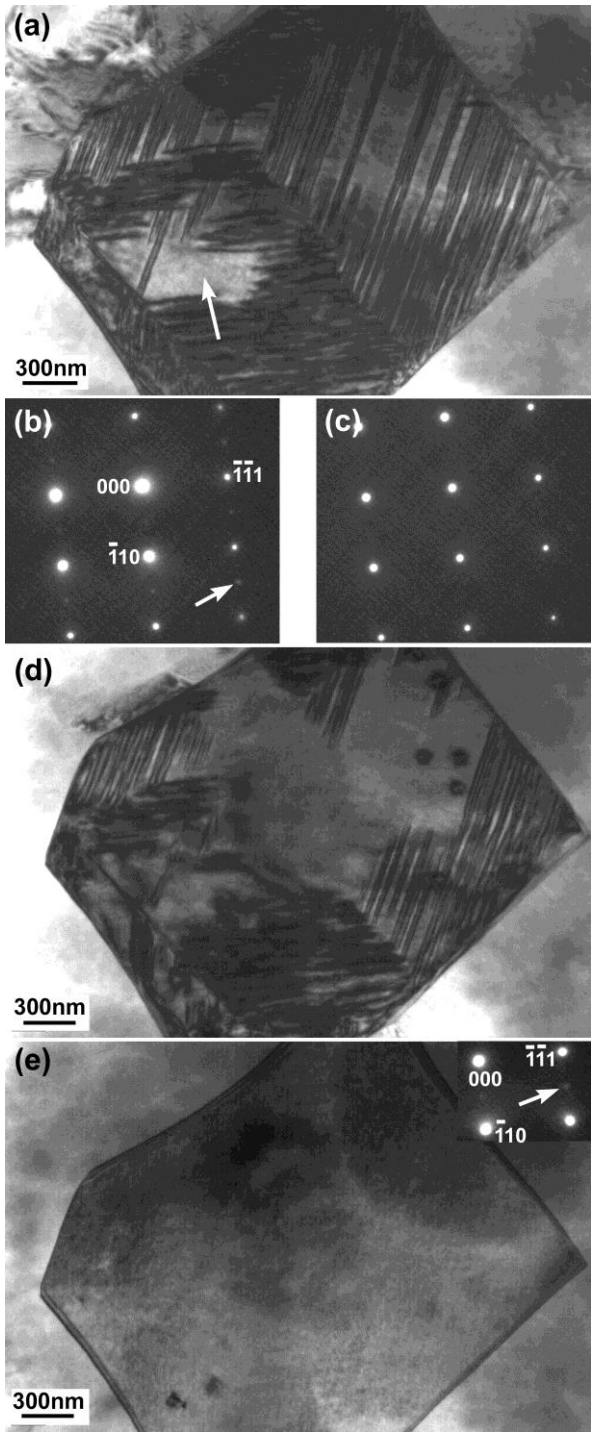
(a)
300nm
(b)
000
$\bar{1}\bar{1}1$
$\bar{1}10$
(c)
(d)
300nm
(e)
000
$\bar{1}\bar{1}1$
$\bar{1}10$
300nm

Fig. 3

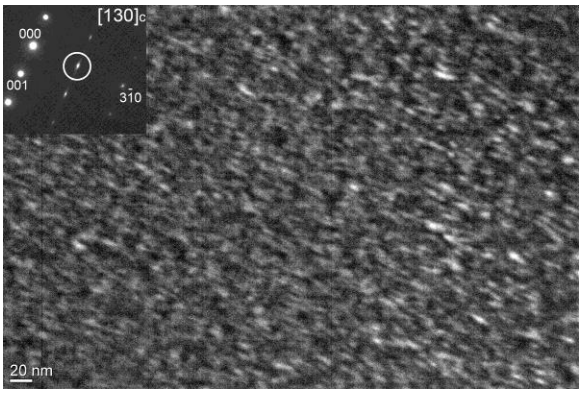

Fig. 4

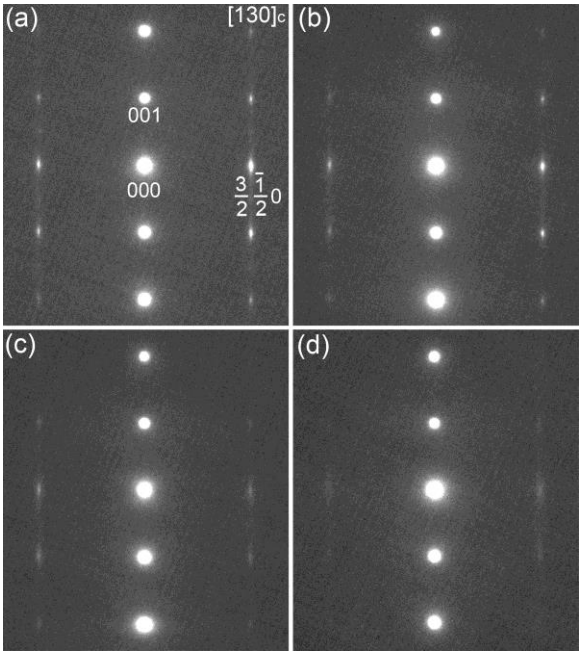

Fig. 5

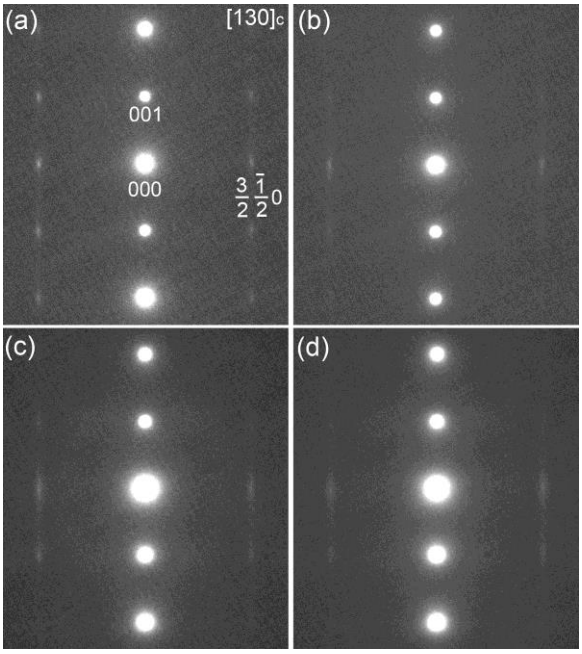

Fig. 6

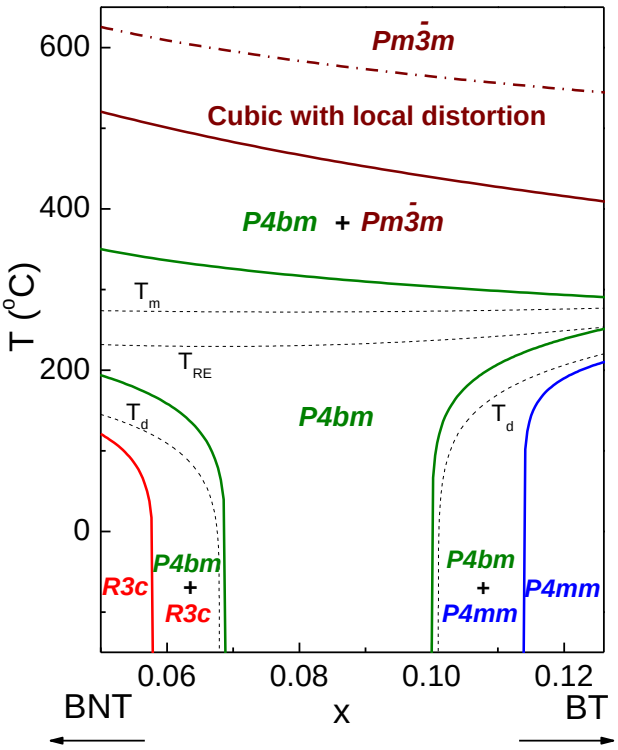
Pm3̄m
Cubic with local distortion
P4bm + Pm3̄m
T (°C)
600
400
200
0
T_m
T_RE
T_d
T_d
P4bm
R3c
P4bm
+
R3c
P4bm
+
P4mm
P4mm
0.06
0.08
0.10
0.12
BNT
x
BT

Fig. 7